








Aerosol and Dimethyl Sulfide Sensitivity to Sulfate Chemistry Schemes

Key Points:

- The simulated spread in aerosol optical depth and cloud droplet number concentration is more than twice as large as the change from pre-industrial to present-day
- Simulations with similar Dimethyl sulfide burdens have very different sulfate burdens driven by the different sulfate mechanisms/oxidation pathways
- Constraining the chemistry of atmospheric sulfur is critical to constrain aerosol-cloud interactions

Yusuf A. Bhatti^{1,2} , Laura E. Revell¹ , Adrian J. McDonald¹ , Alex T. Archibald^{3,4}, Alex J. Schuddeboom^{1,5}, Jonny Williams⁶ , Catherine Hardacre¹, Jane Mulcahy⁷ , and Dongqi Lin^{8,9}

¹School of Physical and Chemical Sciences, University of Canterbury, Christchurch, New Zealand, ²Now at SRON Netherlands Institute for Space Research, Leiden, The Netherlands, ³National Centre for Atmospheric Science, Cambridge, UK, ⁴Yusuf Hamied Department of Chemistry, University of Cambridge, Cambridge, UK, ⁵Now at National Institute of Water and Atmospheric Research (NIWA), Christchurch, New Zealand, ⁶National Institute of Water and Atmospheric Research (NIWA), Wellington, New Zealand, ⁷Met Office, Exeter, UK, ⁸School of Earth and Environment, University of Canterbury, Christchurch, New Zealand, ⁹Now at School of Earth, Atmosphere and Environment, Monash University, Melbourne, VIC, Australia

Supporting Information:

Supporting Information may be found in the online version of this article.

Correspondence to:

Y. A. Bhatti and L. E. Revell,
y.bhatti@srn.nl;
laura.revell@canterbury.ac.nz

Citation:

Bhatti, Y. A., Revell, L. E., McDonald, A. J., Archibald, A. T., Schuddeboom, A. J., Williams, J., et al. (2024). Aerosol and dimethyl sulfide sensitivity to sulfate chemistry schemes. *Journal of Geophysical Research: Atmospheres*, 129, e2023JD040635. <https://doi.org/10.1029/2023JD040635>

Received 18 DEC 2023
Accepted 1 JUN 2024

Abstract Dimethyl sulfide (DMS) is the largest source of natural sulfur in the atmosphere and undergoes oxidation reactions resulting in gas-to-particle conversion to form sulfate aerosol. Climate models typically use independent chemical schemes to simulate these processes, however, the sensitivity of sulfate aerosol to the schemes used by CMIP6 models has not been evaluated. Current climate models offer oversimplified DMS oxidation pathways, adding to the ambiguity surrounding the global sulfur burden. Here, we implemented seven DMS and sulfate chemistry schemes, six of which are from CMIP6 models, in an atmosphere-only Earth system model. A large spread in aerosol optical depth (AOD) is simulated (0.077), almost twice the magnitude of the pre-industrial to present-day increase in AOD. Differences are largely driven by the inclusion of the nighttime DMS oxidation reaction with NO₃, and in the number of aqueous phase sulfate reactions. Our analysis identifies the importance of DMS-sulfate chemistry for simulating aerosols. We suggest that optimizing DMS/sulfur chemistry schemes is crucial for the accurate simulation of sulfate aerosols.

Plain Language Summary Dimethyl sulfide (DMS) is a sulfur-bearing gas predominantly emitted from marine biological activity. DMS is the largest natural contributor to the global sulfur cycle, but its contribution is highly uncertain. Representing the complex chemical conversion of DMS to form natural sulfur atmospheric particles accurately in Earth System Models is difficult. Complex atmospheric chemistry is expensive to implement, therefore simplistic approaches to represent the chemistry are used. Here we examine the variability between different chemistry schemes. To achieve this, we employ a state-of-the-art Earth System Model to compare seven simulations with differing sulfur-related chemical reactions. We show that sulfate chemistry contributes to large uncertainties in aerosol and cloud formation. This work underscores the need to improve sulfur chemistry to improve the accuracy of cloud and aerosol projections in a warming world.

1. Introduction

Dimethyl sulfide (DMS; CH₃SCH₃) is the primary natural source of atmospheric sulfur-containing species (Boucher et al., 2003; Breider et al., 2010). DMS is produced from the biogeochemical activity of marine biota (Bates et al., 1987; Charlson et al., 1987; Keller et al., 1989), and when emitted into the atmosphere, undergoes numerous chemical reactions, some of which lead to the formation of sulfate aerosols (Chen et al., 2018; Hoffmann et al., 2021). Aerosols play an important role in cloud formation and influence Earth's energy balance (Carslaw et al., 2013).

Both natural (biogenic) and anthropogenic emissions contribute to the global sulfur cycle. In the Northern Hemisphere (NH), atmospheric sulfur originates primarily from anthropogenic sources such as power stations and ship emissions (e.g., Smith et al., 2011). In contrast, natural sources dominate atmospheric sulfur loading in the Southern Hemisphere (SH), with anthropogenic sources contributing only 30%–50% (Kloster et al., 2006; Korhonen et al., 2008). Emissions of anthropogenic sulfur-containing gases are well-represented in climate models (Hardacre et al., 2021; Hoesly et al., 2018; Turnock et al., 2020). In contrast, there are significant

© 2024. The Author(s).

This is an open access article under the terms of the [Creative Commons Attribution License](https://creativecommons.org/licenses/by/4.0/), which permits use, distribution and reproduction in any medium, provided the original work is properly cited.

uncertainties regarding natural sulfur emissions, especially over the remote Southern Ocean where DMS emissions are large and observations are sparse (Y. A. Bhatti et al., 2023; Bock et al., 2021; Hulswar et al., 2022).

The Southern Ocean region has a vital role in the global sulfur cycle but is predominately of natural origin, which is one of the largest sources of uncertainty for the sulfur cycle (Fung et al., 2022; Hoesly et al., 2018). This region is where global DMS production maximizes but is poorly constrained in models (Belviso et al., 2004; Bock et al., 2021; Revell et al., 2019), and is closely examined in this work.

Previously we examined the sensitivity of atmospheric DMS to oceanic DMS concentrations and sea-to-atmosphere transfer velocities in a global climate model (Y. A. Bhatti et al., 2023). Here, we examine the sensitivity of sulfate aerosol formation to the model's DMS and sulfate chemistry scheme. Whilst there is active work in the improvement of DMS mechanisms used for modeling (e.g., Cala et al., 2023), current generation climate models use relatively similar DMS and sulfate chemistry schemes, but with slight differences (e.g., Archibald et al., 2020; Horowitz et al., 2020; Sheng et al., 2015). We implemented seven such well-established chemistry schemes taken from other CMIP6 climate models into a single model and assessed uncertainties in aerosol and cloud properties associated with sulfate chemistry. As recent discoveries in sulfate chemistry have not been implemented within the CMIP climate model chemistry schemes, we have chosen to exclude them for a more focused evaluation of the chemistry schemes. Model configurations and simulation descriptions are described in Section 2, and results are shown in Section 3.

2. Methods

2.1. Model Configuration and Simulations Performed

Simulations were performed with the atmosphere-only configuration of the UK Earth System Model (UKESM1-AMIP), which operates on a grid with a resolution of 1.25° latitude \times 1.85° longitude (Sellar et al., 2019). All simulations were performed with the oceanic DMS data set "MODIS-DMS" calculated from satellite chlorophyll *a* observations, which is described and evaluated by Y. A. Bhatti et al. (2023). DMS emissions are calculated using the transfer velocity from Blomquist et al. (2017). Atmospheric oxidation of DMS is handled via the StratTrop chemistry scheme (labeled here as "REF"; Archibald et al., 2020; Mulcahy et al., 2020), which is modified for the sensitivity simulations.

StratTrop comprises 84 chemical species and 266 chemical reactions. The O_x , HO_x , and NO_x cycles are included within StratTrop, with their own production and loss mechanisms. Sea-salt aerosol debromination from tropospheric bromine radical chemistry and chloride mobilization is absent in the UKESM1, unlike in other models such as GEOS-Chem. Methanesulfonic acid (MSA), which is produced by DMS reacting with OH, is treated as a sink for DMS in UKESM1-AMIP and is not transported or advected (Mulcahy et al., 2020). MSA does not oxidize to form or contribute to aerosol formation.

Aerosol microphysics is determined using the Global Model of Aerosol Processes (GLOMAP-mode)—a two-moment modal aerosol microphysics scheme. This scheme simulates various aerosol species across five lognormal size modes: nucleation mode, soluble Aitken mode, accumulation mode, coarse mode, and insoluble Aitken mode (Mulcahy et al., 2020). Typically, aerosols with a radius of ≥ 25 nm (Aitken mode) are activated into cloud condensation nuclei (CCN) and cloud droplets (Abdul-Razzak & Ghan, 2000; Walters et al., 2019). A constant cloud water pH of 5.0 is used in the UKESM1, which is important for aqueous-phase chemistry (Turnock et al., 2019). Greenhouse gas concentrations and anthropogenic aerosol emissions follow Coupled Model Intercomparison Project Phase 6 (CMIP6) recommendations.

Simulations were run for three years, from January 2016 to December 2018, with the first year discarded as spin-up. Wind and temperature are nudged to values from the ERA-5 reanalysis at 6-hourly intervals (Dee et al., 2011; Hersbach et al., 2020).

Six sensitivity simulations were performed using DMS and sulfate chemistry schemes from other Earth system models, most of which participated in CMIP6 (Table 1). Some of the CMIP6 models use very similar sulfate chemistry schemes, so not all CMIP6 models are represented, to avoid duplication. For detailed DMS and non-DMS sulfur reactions, refer to Tables S1 and S2 in Supporting Information S1. In terms of gas-phase chemistry, all schemes feature an OH addition and abstraction pathway. All schemes also include a NO_3 oxidation reaction for DMS, except MIROC. None include the newly identified hydroperoxymethyl thioformate (HPMTF), a DMS

Table 1
Chemical Reactions Used in Each Simulation

Chemical reaction	REF	SEN-SOCOL ^a	SEN-MIROC ^b	SEN-GFDL ^c	SEN-GEOS-Chem ^d	SEN-CHEM3	SEN-NorESM ^e
DMS + OH (abs)	Light gray	Light gray	Light gray	Light gray	Light gray	Light gray	Light gray
DMS + OH (add)	Light gray	Light gray	Light gray	Light gray	Light gray	Light gray	Light gray
DMS + NO ₃	Light gray	Light gray	Light gray	Light gray	Light gray	Light gray	Light gray
DMS + ClO	Light gray	Light gray	Light gray	Light gray	Light gray	Light gray	Light gray
DMS + Br	Light gray	Light gray	Light gray	Light gray	Light gray	Light gray	Light gray
DMS + BrO	Light gray	Light gray	Light gray	Light gray	Light gray	Light gray	Light gray
DMS + O ₃	Light gray	Light gray	Light gray	Light gray	Light gray	Light gray	Light gray
DMS + O(³ P)	Light gray	Light gray	Light gray	Light gray	Light gray	Light gray	Light gray
DMS + Cl	Light gray	Light gray	Light gray	Light gray	Light gray	Light gray	Light gray
DMS(aq) + O ₃ (aq)	Light gray	Light gray	Light gray	Light gray	Light gray	Light gray	Light gray
SO ₂ + OH	Medium gray	Medium gray	Medium gray	Medium gray	Medium gray	Medium gray	Medium gray
SO ₂ + O	Medium gray	Medium gray	Medium gray	Medium gray	Medium gray	Medium gray	Medium gray
SO ₂ + O ₃	Medium gray	Medium gray	Medium gray	Medium gray	Medium gray	Medium gray	Medium gray
SO ₃ + H ₂ O	Medium gray	Medium gray	Medium gray	Medium gray	Medium gray	Medium gray	Medium gray
DMSO + OH	Medium gray	Medium gray	Medium gray	Medium gray	Medium gray	Medium gray	Medium gray
MSIA + O ₃	Medium gray	Medium gray	Medium gray	Medium gray	Medium gray	Medium gray	Medium gray
MSIA + OH	Medium gray	Medium gray	Medium gray	Medium gray	Medium gray	Medium gray	Medium gray
S(IV) + H ₂ O ₂ (aq)	Dark gray	Dark gray	Dark gray	Dark gray	Dark gray	Dark gray	Dark gray
SO ₃ ²⁻ + O ₃ (aq)	Dark gray	Dark gray	Dark gray	Dark gray	Dark gray	Dark gray	Dark gray
HSO ₃ ⁻ + O ₃ (aq)	Dark gray	Dark gray	Dark gray	Dark gray	Dark gray	Dark gray	Dark gray
HSO ₃ ⁻ + HOBr(aq)	Dark gray	Dark gray	Dark gray	Dark gray	Dark gray	Dark gray	Dark gray
SO ₃ ²⁻ + HOBr(aq)	Dark gray	Dark gray	Dark gray	Dark gray	Dark gray	Dark gray	Dark gray
O ₃ (aq) + MSI ^{-c} (aq)	Dark gray	Dark gray	Dark gray	Dark gray	Dark gray	Dark gray	Dark gray
O ₃ (aq) + MSIA(aq)	Dark gray	Dark gray	Dark gray	Dark gray	Dark gray	Dark gray	Dark gray
S(IV) + HO ₂ NO ₂ (aq)	Dark gray	Dark gray	Dark gray	Dark gray	Dark gray	Dark gray	Dark gray

Note. Light gray shading: DMS oxidation reactions. Medium gray shading: gas-phase reactions involving DMS oxidation products. Dark gray shading: aqueous phase reactions involving sulfur-containing species. All reactions are gas-phase unless otherwise indicated. All models contain two DMS + OH reactions; abstraction and addition. For reaction rates and references see Tables S1 and S2 in Supporting Information S1. ^aSolar-climate Ozone Links (SOCOL). ^bModel for Interdisciplinary Research on Climate (MIROC). ^cGeophysical Fluid Dynamics Laboratory (GFDL). ^dGoddard Earth Observing System (GEOS). ^eNorwegian Earth System Model (NorESM).

oxidation product (Veres et al., 2020), although its role is actively researched (Cala et al., 2023; Fung et al., 2022). All schemes involve at least two aqueous-phase in-cloud reactions. StratTrop, CHEM3, and GEOS-Chem have a third aqueous-phase reaction with O₃. CHEM3 is the only scheme absent from a CMIP6 model and is used here to represent a more complex and realistic chemistry scheme, described by Chen et al. (2018) and Revell et al. (2019). GEOS-Chem and CHEM3 have the largest number of aqueous-phase reactions (Chen et al., 2016, 2017; Revell et al., 2019). Differences between each model tuning mean that the spread between chemistry schemes will be smaller if doing an intercomparison using their own model. Here we go further than just testing expansions of sulfate chemistry schemes, but quantifying how much variability in DMS and aerosol can result just from using CMIP6-based or well-established chemistry schemes.

The most recent advances in sulfate chemistry, including HPMTF, are not implemented within the CMIP6 chemistry schemes. These advances are being studied and evaluated (Cala et al., 2023), with observations still lacking for many parts of the world. Therefore, we have excluded them and focused our evaluation on the spread between the chemistry schemes used within CMIP6 models.

We quantify the spread between the simulations in the values derived from the various chemistry schemes using the relative range in percentage. This is calculated by the difference between the largest and smallest values, divided by the smallest value, and then multiplied by 100.

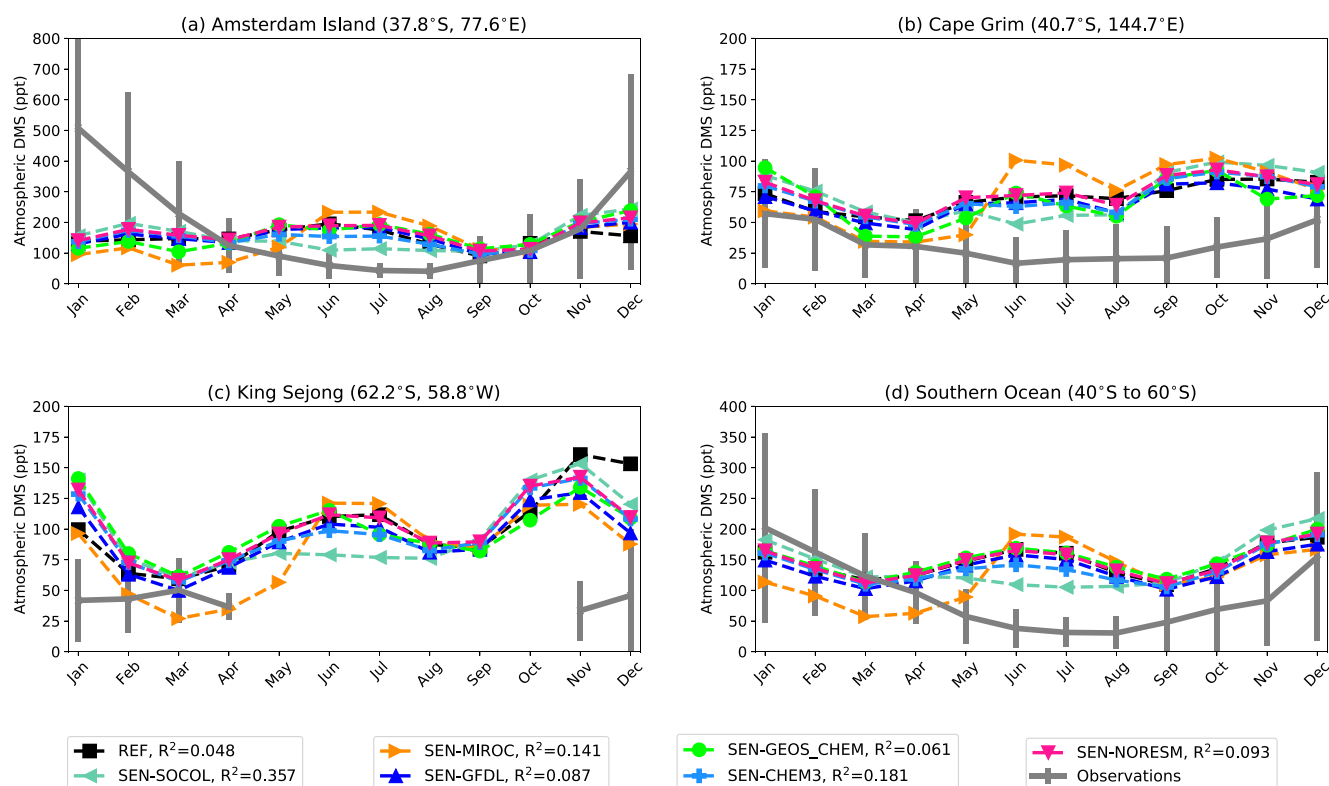


Figure 1. Southern Ocean atmospheric Dimethyl sulfide surface concentrations showing climatological monthly means for the simulations comparing differing sulfate chemistry schemes with observations. Lines show the observational means (in gray) and their standard deviation (error bars) compared with the simulations for the same grid cells. The Southern Ocean measurements are compiled from three ground-based stations and four voyages, all weighted equally. The average R^2 value represents the seasonal correlation coefficient between the simulation and each respective observation.

2.2. Observational Data Sets

Satellite, ground, and ship-based observations were used for model evaluation (Table S3 in Supporting Information S1). Data from the Southern Ocean, representing a region largely untouched by anthropogenic aerosol emissions, are limited. To evaluate atmospheric DMS in this region we merge ground and ship-based data into one data set, each weighted equally across each month. Only two sources offer DMS data for the Austral winter, but the summer and autumn are represented by seven data sets (Table S3 in Supporting Information S1).

3. Results and Discussion

The Southern Ocean (40°S to 60°S) is a focus of this study to investigate the different sulfate chemistry schemes used in the model simulations, and to compare with observations of atmospheric DMS. Our simulations highlight a global significance in the production of DMS from the Southern Ocean, as 49%–70% of the global atmospheric DMS burden originates from this region.

Average DMS concentrations are relatively well constrained between the simulations, which is unsurprising given that all simulations used the same oceanic DMS source and sea-to-air transfer velocity. Previous work has evaluated DMS and other aerosol properties in UKESM1-AMIP (Y. A. Bhatti et al., 2023; Mulcahy et al., 2020). Y. A. Bhatti et al. (2023) identified a 171% spread in DJF atmospheric DMS from Southern Ocean DMS concentrations and emissions, whereas the spread identified from the simulations performed here during the same period and region is 48%. Although the emissions and concentrations drive much of the spatial and seasonal variability of atmospheric DMS, we demonstrate that differences in CMIP6 chemistry also have a profound influence on Southern Ocean atmospheric DMS. Here we examine the seasonal cycle in DMS from available observations (Figure 1).

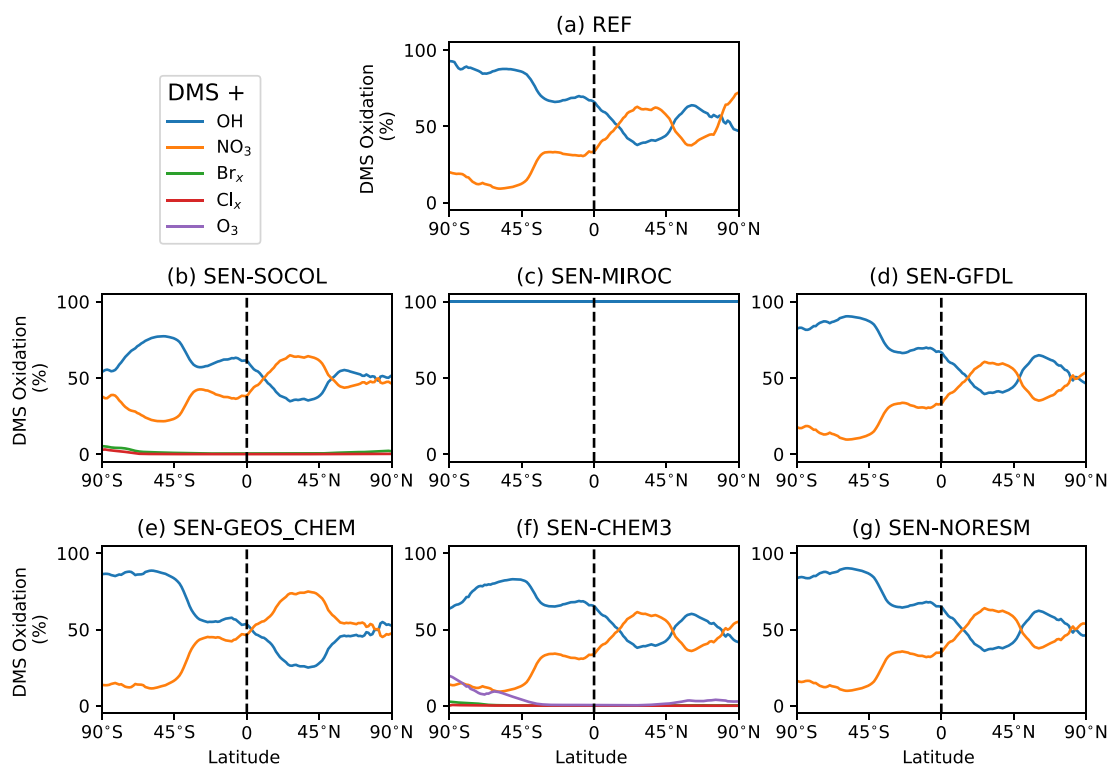


Figure 2. Zonal annual means of the relative proportions of all chemical reactions (%) involved in Dimethyl sulfide oxidation. The sum of all reactions for each simulation equals 100%. The dashed line indicates the equator. Br_x = Br and/or BrO and Cl_x = Cl or ClO. See Table 1 for more details.

As shown in Figure 1, all simulations overestimate austral wintertime (JJA) atmospheric DMS but generally are closer to observations in summer months, except at Amsterdam Island. The year-long observational stations display a clear seasonal cycle for Southern Ocean DMS; however, none of the simulations successfully capture the DMS depletion during winter. This could be because the UKESM1 lacks a tropospheric BrO and ClO source from sea-spray, which has been identified as a significant loss of DMS during the winter (Breider et al., 2010; Fung et al., 2022). The SOCOL chemistry scheme enables UKESM1-AMIP to best represent the seasonal cycle in atmospheric DMS ($R^2 = 0.357$ compared to observations; $R^2 < 0.2$ for all other simulations).

The current representation of the UKESM1-AMIP Southern Ocean DMS may be flawed during the wintertime, as demonstrated by increases in DMS concentrations which do not occur in any observations (Figure 1). DMS is mostly oxidized via NO_3 during austral winter, however, most simulations do not oxidize DMS quickly enough, resulting in an accumulation of DMS during winter from the less efficient wintertime loss pathway, which SEN-SOCOL shows. Including a Cl and Br tropospheric chemistry source may improve the representation of DMS oxidation in UKESM1, and possibly mitigate DMS biases over the Southern Ocean. The additional Cl and Br chemistry is an important source for DMS oxidation during winter, in agreement with Chen et al. (2018). Although the distribution of atmospheric DMS is mostly controlled by the oceanic DMS and DMS emissions (Y. A. Bhatti et al., 2023), we demonstrate the importance of choosing a sulfate chemical reaction scheme appropriately over the Southern Ocean. As a result, we investigate the global differences in chemical oxidation of DMS between each simulation.

3.1. Chemical Oxidation of DMS

Globally, DMS + OH reactions account for 56%–65% of total DMS loss in our simulations (Figure 2), in agreement with Fung et al. (2022). DMS oxidation via the OH addition and abstraction pathways dominates other oxidation reactions in the SH, while DMS + NO_3 is largest in the NH where there are large anthropogenic NO_x emissions. The hemispheric distribution of the widely used DMS reactions (DMS + OH and DMS + NO_3) is consistent with Chen et al. (2018). The contribution of DMS + NO_3 to global DMS loss is approximately 35%–42% (Figure 2), similar to prior estimates between 16% and 45% (Kloster et al., 2006; Mulcahy et al., 2020).

Global DMS lifetimes of 1.2–1.4 days are consistent with the literature estimates of 0.72–2.34 days (Breider et al., 2010; Mulcahy et al., 2020). SEN-SOCOL (Figure 2b and Figure S1b in Supporting Information S1) has more DMS oxidized by NO_3 at the high SH latitudes than the other chemistry schemes, therefore reducing the lifetime of DMS, especially during winter. This reduces the relative importance of DMS oxidation via OH.

In SEN-GEOS-Chem, there is more DMS oxidation by NO_3 over the NH than in the other simulations (Figure 2e and Figure S1e in Supporting Information S1). SEN-MIROC, without a DMS + NO_3 reaction, lengthens the DMS lifetime over high northern latitudes (not shown), in contrast to the other simulations. However, SEN-MIROC contains an alternative DMS loss pathway via DMSO, and essentially becomes a night loss mechanism for DMS (not shown), compensating for the lack of DMS + NO_3 reaction.

The inclusion of additional DMS oxidation pathways (e.g., ozone, reactive chlorine, and bromine) as in SOCOL and CHEM3 has a relatively minor impact on DMS oxidation. UKESM1-AMIP currently only has a stratospheric source of inorganic chlorine or bromine, which explains why the contribution of these pathways is close to zero in Figures 2b and 2f. Future work will investigate the impacts on sulfur chemistry by implementing tropospheric inorganic chlorine and bromine sources.

The treatment of MSA varies largely across each CMIP6 model, with some models producing no MSA. GEOS-Chem and NorESM allow for MSA to oxidize into aerosol (Chin et al., 1996; Kirkevåg et al., 2013) whereas StratTrop and SOCOL only provide a wet/dry removal mechanism for MSA (Feinberg et al., 2019; Mulcahy et al., 2020). The extent of divergence between models in their treatment of MSA is surprising, given that the existence of MSA and its oxidizing potential has long been known (Charlson et al., 1987; Lovelock et al., 1972). More recent studies have quantified MSA to have a significant contribution to aerosol, especially in the Southern Ocean region (Chen et al., 2018; Fung et al., 2022). There is a clear divide between the most recent advances in sulfate chemistry schemes compared with those implemented within CMIP6. The current advances in extended sulfate chemistry schemes focus on the implementation of HPMTF (Cala et al., 2023; Tashmim et al., 2024). However, chemistry schemes within CMIP6 models still diverge away from each other in the treatment of MSA. Therefore, we suggest that CMIP7 models have a chemical removal mechanism of MSA, to better represent recent advances in sulfate chemistry.

Our results show minor differences in DMS lifetime and concentrations when comparing simulations with up-to-date rate constants (Burkholder et al., 2020) to those without (Figures 1 and 2). We, therefore, suggest that other modeling groups regularly ensure rate constant parameters are up-to-date to have more accurate DMS reactions. Expanding the analysis to other sulfur species, including DMS, which are instrumental toward aerosol formation is further evaluated below.

3.2. Aerosol Response to Sulfate Chemistry Schemes

To better understand the differences in aerosol between the simulations with differing sulfate chemistry, we examine the aerosol modes, CCN and H_2SO_4 concentrations. Number concentrations of aerosol in different modes from our simulations are shown in Figure 3 (a–c for NH, g–i for SH). We exclude coarse mode aerosols which are dominated by sea spray in UKESM1-AMIP.

The aerosol number size distribution in the NH is around three times higher than in the SH for each aerosol mode, except coarse (Figures 3f and 3l). The coarse mode ($\geq 0.25 \mu\text{m}$), which consists mainly of primary aerosols such as sea-spray (Mulcahy et al., 2020; Revell et al., 2019), is not considered in this study due to its low anthropogenic influence. To better understand the global influences and vulnerability of these aerosol modes to the chemistry schemes within Earth System Models, future work should assess the natural and anthropogenic contribution toward each aerosol mode.

The annual mean spread in the nucleation mode (Figure 3a) in the NH is more than double that of the Aitken (Figure 3b) and accumulation (Figure 3c) modes. This aligns with Fiddes et al. (2018), emphasizing that the nucleation mode has the highest sensitivity to sulfur sources. However, the difference between the nucleation mode and the other modes is not as great in the SH as in the NH, which is due to the different sulfur sources between the hemispheres. The simulations show more significant differences in the NH than in the SH, with the NH containing 129% more nucleating particles (Figures 3a, 3g, 3f, and 3l), which is similar to the findings from Minikin et al. (2003). Additionally, H_2SO_4 has much higher concentrations over the NH. These hemispheric

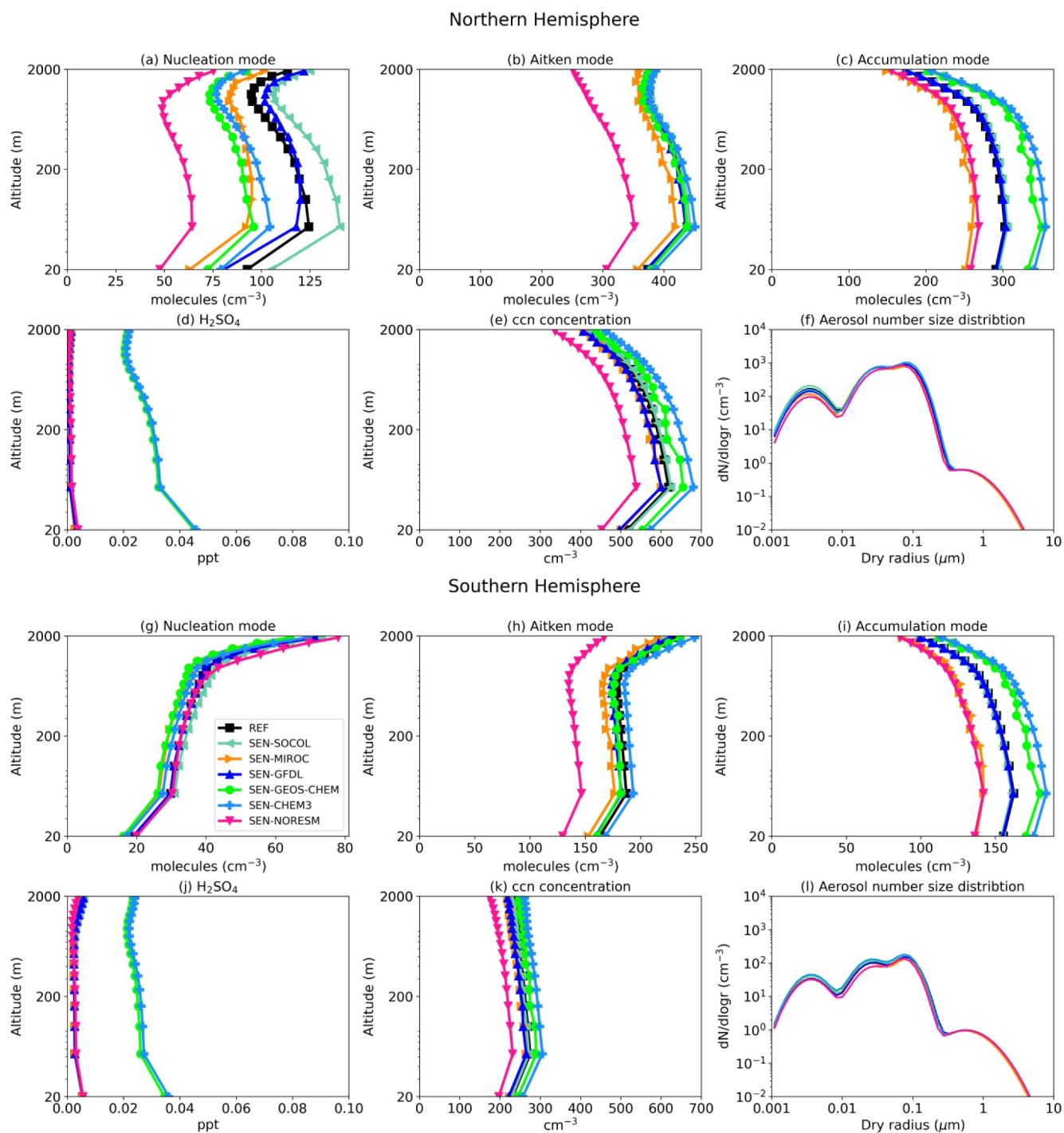


Figure 3. Northern and Southern Hemisphere averaged aerosol number concentrations from the (a, g) nucleation-mode, (b, h) Aitken-mode, (c, i) accumulation-mode. (d, j) The H_2SO_4 abundance is shown in parts per trillion (ppt). (e, k) Cloud condensation nuclei and (f, l) Global aerosol number size distributions are also shown. (a–f): Northern Hemisphere average; (g–l): Southern Hemisphere average.

contrasts suggest that sulfur over the NH has a much greater sensitivity to changes in the sulfate chemistry than sulfur over the SH.

In both the NH and SH SEN-NorESM has lower Aitken and accumulation mode concentrations compared to most of the other simulations which leads to lower AOD and CCN. This can be attributed to the scheme using only one

SO₂ oxidation pathway, reducing atmospheric sulfate available for conversion to aerosol. As aerosols grow from the nucleation mode, they have a greater influence on cloud formation (Figures 3e and 3k). SEN-GEOS-Chem and SEN-CHEM3 have the highest CCN concentrations due to larger concentrations of H₂SO₄. Simulations with more aqueous-phase chemistry may allow more sulfate aerosol to transfer into larger aerosol modes. For example, shown in Figure 3a, the SEN-GEOS-Chem and SEN-CHEM3 simulations contain fewer nucleation mode aerosol concentrations than the REF simulation. However, SEN-GEOS-Chem and SEN-CHEM3 contain the highest concentrations within the larger modes (Figures 3c and 3i).

Accurately representing cloud-water pH in climate models is crucial for aqueous-phase chemistry and cloud formation (Turnock et al., 2019). Global cloud water pH varies between 3 and 8, however, UKESM1 uses a uniform value of 5 (Shah et al., 2020). A small increase in pH could reduce the number of aerosols serving as CCN (Turnock et al., 2019). Chemistry schemes used in their native models are effectively tailored to that model's specific configurations. For example, GEOS-Chem has interactive cloud-water pH affecting aerosol modes differently to the UKESM1 (Alexander et al., 2012). Other models, like GFDL, assume cloud water pH of 4.5, leading to differences in their aqueous-phase reactions (Krasting et al., 2018; Turnock et al., 2016). DMS oxidation into SO₄²⁻ can also impact pH (Shah et al., 2020), particularly in DMS-rich areas like the Southern Ocean. Excessive oxidation can lower the pH, impacting cloud formation. Thus, assuming a uniform cloud-water pH for the Southern Ocean will lead to model spread, given the significant oxidation variations across simulations. Further work in updating the UKESM1 chemistry sources is therefore needed to better represent aerosols and DMS. For instance, the inclusion of a BrO inorganic source from sea-spray would provide a much greater avenue for DMS oxidation during the winter, which has been shown to have a substantial impact (Breider et al., 2010; Fung et al., 2022).

3.3. Sensitivity to Sulfate Chemistry Schemes

To assess the overall sensitivity of sulfate formation to atmospheric chemistry, we analyze simulated DMS, AOD, cloud droplet number concentration (CDNC), and all-sky shortwave radiation at the top of the atmosphere relative to the SO₄²⁻ mass fraction (which is integrated between the surface and top-of-atmosphere; Figure 4).

The spread between all the simulations annual mean is 20% for DMS globally. The DMS burden is reasonably well constrained (ranging between 35 and 44 Gg S globally (Figure 4a)). The vertical error bars are larger in the SH than in the NH because of the large seasonality in marine biogenic activity at southern high latitudes (Figures 4e and 4i; Curran & Jones, 2000; Jarníková & Tortell, 2016). With the exception of the MIROC scheme, the spread is 12% in DMS burden across the models. The MIROC chemistry scheme omits the DMS + NO₃ oxidation reaction, which is important in the removal of DMS over the NH due to anthropogenic nitrate emissions (Archer-Nicholls et al., 2023; Chen et al., 2018).

DMS has a more pronounced effect on all sulfur sources in the SH than in the NH. The global contribution of atmospheric DMS to the overall sulfur burden (DMS_{sulfur}) across all simulations is shown in Table S4 in Supporting Information S1. Around 80% of the global annual average DMS_{sulfur} is sourced entirely from SH annual average DMS (Table S4 in Supporting Information S1). The primary sulfur source in the NH is anthropogenic SO₂ emissions which contribute to 75% of the global SO₂ burden, from the REF simulation (not shown), similar to other estimates (Smith et al., 2011). The contribution of DMS produced within the NH to the entire global sulfur burden ranges between 1.8% and 5.1%, as shown in Table S4 in Supporting Information S1. In contrast, the SH, characterized by extensive regions devoid of anthropogenic emissions, has higher proportions of natural sulfur emissions (Y. Bhatti et al., 2022; Gondwe et al., 2003; Hamilton et al., 2014; Kloster et al., 2006; McCoy et al., 2020). As a result, we find that between 10% and 21% of global sulfur is sourced from SH DMS (refer to Table S4 in Supporting Information S1). Previous estimations for the contribution of DMS to the hemispheric sulfur burden are generally close to the range of our study (6.5% and 18.5% from the NH and SH, respectively; Kloster et al., 2006). Kloster et al. (2006) and Gondwe et al. (2003) place a higher importance on NH DMS as a sulfur source than our simulations generally do. Gondwe et al. (2003) use the climatology of Kettle et al. (1999), which contains a 10%–14% higher proportion of global oceanic DMS within the NH than in Lana et al. (2011) or Hulswar et al. (2022) which promotes higher DMS burdens over the NH. Kloster et al. (2006) use an interactive biogeochemical model which includes DMS sea surface concentration measurements from the Kettle and Andreae (2000) database that produces even greater NH DMS emissions than Kettle et al. (1999).

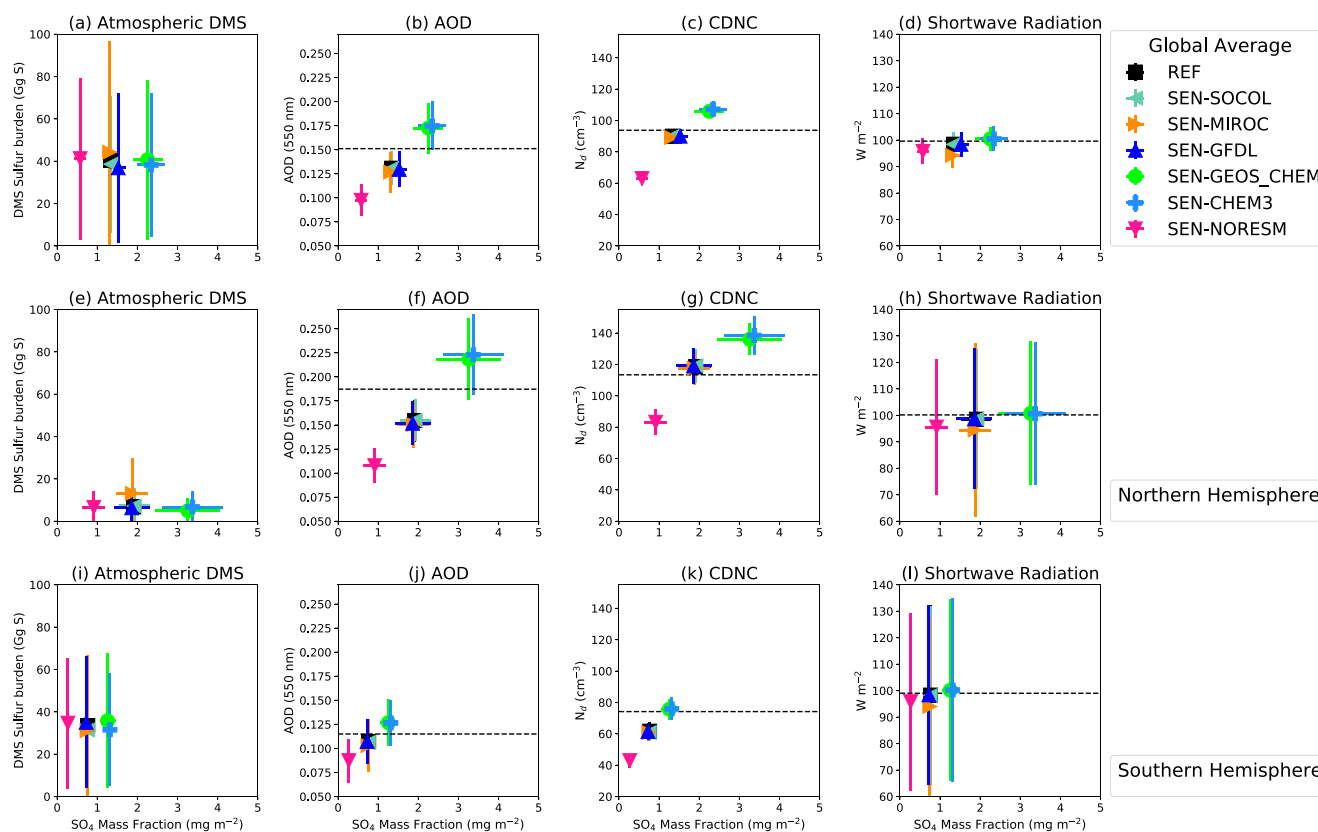


Figure 4. Annual-mean atmospheric Dimethyl sulfide (DMS) sulfur burden, aerosol optical depth (AOD), cloud droplet number concentration (CDNC), and shortwave radiation as a function of the vertically integrated SO_4^{2-} mass fraction. Top row: global average; middle row: Northern Hemisphere (NH); bottom row: Southern Hemisphere (SH). The dashed horizontal line represents the average value from observations. First column: atmospheric DMS (no global observations are available); second column: MODIS AOD (Platnick et al., 2017); third column: CDNC satellite measurements at cloud top between 2017 and 2018 from Grosvenor et al. (2018); fourth column: TOA all-sky shortwave radiation from CERES (Loeb et al., 2018). Error bars show the standard deviation on spatially averaged quantities calculated over the 2-year simulations. The DMS burden is the sum of global sulfur from DMS, over the SH (panel (i)) and NH (panel (e)) DMS burden, for each simulation, respectively (panel (a)).

Figures 4a, 4e, and 4i demonstrates that simulations with very similar DMS burdens have very different SO_4^{2-} burdens driven by the different sulfate mechanisms/oxidation pathways. The spread in the global annual mean SO_4^{2-} mass fraction across the simulations is 308%. SO_4^{2-} is crucial for the formation of clouds and aerosol (Figure 4) and consequently global annual mean AOD and CDNC have a spread of 79% (0.077) and 70% (44 cm^{-3}) across our simulations (Figures 4b and 4c). However, when excluding SEN-NorESM, this spread constricts to just 38% for AOD and 20% for CDNC. The spread in AOD between our simulations is much greater than the AOD of 0.031 from CMIP6 models (Vogel et al., 2022). Additionally, global annual mean AOD is suggested to have only increased by 0.04–0.046 since pre-industrial times, with CDNC also increasing by 10–20 cm^{-3} , highlighting the large variation between the chemistry schemes (Bauer et al., 2020; Y. Bhatti et al., 2022; Kirkevåg et al., 2018; Seo et al., 2020; Tsigaridis et al., 2006).

The spread of the simulations' annual mean between both hemispheres is the same for CDNC but is two times greater over the NH than the SH for AOD. This implies that the variance in AOD is driven more by anthropogenic sulfur than DMS. We also find that due to the increased anthropogenic SO_2 emissions over the NH, sulfate aerosol, AOD, and CDNC concentrations are all much greater over the NH (Figures 3 and 4). Similarly, (McCoy et al., 2020) found large hemispheric differences in radiative forcing due to the contrasting concentrations and distributions in clouds and aerosol between the more polluted NH compared with the SH.

For all simulations, there is a linear relationship between AOD and CDNC versus SO_4^{2-} mass fraction: the chemistry schemes that oxidize DMS and sulfate more efficiently (such as SEN-GEOS-Chem and SEN-CHEM3) also produce more AOD and CDNC. All simulations showing AOD and CDNC over the SH are closer to the

observed AOD and CDNC averages. Future work will quantify what fraction of the spread in aerosol is driven by DMS and from anthropogenic sulfur. Although DMS is the dominating source of natural sulfur (Szopa et al., 2021), other natural sulfur sources have a large influence on the climate, including volcanoes (Neely & Schmidt, 2016) and biomass burning (van Marle et al., 2016). Both were represented by the same set of emissions in the CMIP6 simulations, as in our simulations.

SEN-NorESM has the lowest AOD, CDNC, and SO_4^{2-} mass fraction, but an average DMS burden. This is likely due to inefficient sulfur-to-aerosol conversion over the NH demonstrated by a higher sulfur burden and fewer reactions involving SO_4^{2-} products than other schemes (Table S2 in Supporting Information S1). More specifically, the lower aerosol likely results from decreased SO_4^{2-} mass fraction (Figure 4) and less efficient SO_2 oxidation into H_2SO_4 , as discussed in Section 3.2.

The CHEM3 scheme is a modified version of the SEN-GEOS-Chem DMS and sulfate chemistry scheme, with both simulations simulating the largest global CDNC (Chen et al., 2018; Revell et al., 2019). Revell et al. (2019) showed that SEN-CHEM3 leads to increased CDNC over the Southern Ocean due to the inclusion of additional aqueous-phase sulfate reactions. Despite pronounced differences in global mean CDNC ($63\text{--}107\text{ cm}^{-3}$, Figure 4c), differences in top-of-atmosphere all-sky shortwave radiation are relatively small between the simulations (Figures 4d, 4h, and 4l).

4. Summary and Conclusions

This study compares the differences between sulfate chemistry schemes using identical base configurations. The sensitivity of DMS and its oxidation products to changes in sulfate chemistry was investigated using a nudged configuration of the UKESM1-AMIP model. We show that testing 7 sulfate chemistry schemes in one model causes large variations in SO_4^{2-} , CNDC, and AOD across simulations; twice the change in AOD and CDNC between the pre-industrial and the present-day when simulated in UKESM1 (Bauer et al., 2020; Seo et al., 2020). Additional aqueous-phase chemistry increases the inter-model variance through an increased number of larger aerosols. Our results need further investigation to determine if they would be universally robust. For example, because of differences in model formulation (grid box sizes, oxidant levels and many other processes), we don't expect the same sensitivities we have calculated here across other "base models"—and we encourage work that would address this issue as a priority. As each model treats DMS and sulfur chemistry and aerosol microphysical processes differently from UKESM1, such as differences in cloud water pH or aerosol size distributions, the spread in AOD (0.077) is more than double that compared between CMIP6 simulations (0.031; Vogel et al., 2022). Therefore, careful consideration is necessary when modifying sulfate chemistry schemes in climate models as aerosol response may vary significantly. We highlight the associated uncertainty to aerosol and CDNC from sulfate chemistry seems to be significantly large enough that it may alter the pre-industrial baseline and therefore be an important source of uncertainty in aerosol ERF estimates. Therefore our study builds on previous perturbed parameter ensemble studies of aerosol parameters which did not consider these parameters (Carslaw et al., 2013).

We demonstrate that differences between well-established DMS and sulfate aerosol chemistry schemes can strongly impact the global spread of DMS concentrations by as much as 20% between the simulations, with larger fluctuations over the NH. These global differences arise from differences in DMS oxidation pathways. Large seasonal differences are also present between the simulations over the Southern Ocean, with the closest simulation to observations coming from the SOCOL chemistry scheme (R^2 of 0.36). The UKESM1-AMIP currently lacks an inorganic BrO source from sea-spray which may provide improvements to comparisons with observations, especially during the winter. The spread in Southern Ocean DJF atmospheric DMS associated with chemistry (48%) is less than the spread from oceanic concentration and emissions (171%).

This work demonstrates the importance of DMS and sulfate chemistry in future model intercomparison projects for future aerosol modeling. The necessity for additional mechanistic studies and model validation is highlighted in this study. Sulfur chemistry, including recent discoveries, should be accurately incorporated into the model. As these chemistry schemes evolve for CMIP7, becoming more computationally demanding, these schemes will likely increase in diversity and may result in a greater spread. Current chemistry schemes, tested in this work, lack realistic or comprehensive chemistry which therefore may enhance the current uncertainty in DMS oxidation

chemistry, demonstrated in this work. Overall, we find that testing different sulfate chemistry schemes in a single model can strongly affect aerosols and cloud formation.

Data Availability Statement

The MODIS-aqua satellite data from AOD and chlorophyll *a* are available in <https://giovanni.gsfc.nasa.gov/giovanni/>. Cloud droplet number concentration observational data are available from <https://doi.org/10.5285/864a46cc65054008857ee5bb772a2a2b>. The CERES data was obtained in <https://ceres.larc.nasa.gov/data/>. Dimethyl sulfide measurements are available at <https://ebas-data.nilu.no/Default.aspx>. Model simulation data are archived at New Zealand eScience Infrastructure (NeSI; <https://www.nesi.org.nz/>). As all simulation data is over 1 Terabyte, they will be managed and made available for at least 5 years by contacting the corresponding author.

Acknowledgments

This research was supported by the Deep South National Science Challenge (Grants C01X141E2 and C01X1901). We acknowledge the UK Met Office for the use of the UM. We also acknowledge the contribution of NeSI high-performance computing facilities to the results of this research. New Zealand's national facilities are provided by NeSI and funded jointly by NeSI's collaborator institutions and through the Ministry of Business, Innovation and Employment's Research Infrastructure programme (<https://www.nesi.org.nz/>). We acknowledge the Cape Grim Science Program for the provision of DMS data from Cape Grim. The Cape Grim Science Program is a collaboration between the Australian Bureau of Meteorology and the CSIRO Australia. LER appreciates support by the Rutherford Discovery Fellowships from New Zealand Government funding, administered by the Royal Society Te Apārangi. Open access publishing facilitated by University of Canterbury, as part of the Wiley - University of Canterbury agreement via the Council of Australian University Librarians.

References

- Abdul-Razzak, H., & Ghan, S. J. (2000). A parameterization of aerosol activation: 2. Multiple aerosol types. *Journal of Geophysical Research*, *105*(D5), 6837–6844. <https://doi.org/10.1029/1999JD901161>
- Alexander, B., Allman, D. J., Amos, H. M., Fairlie, T. D., Dachs, J., Hegg, D. A., & Sletten, R. S. (2012). Isotopic constraints on the formation pathways of sulfate aerosol in the marine boundary layer of the subtropical northeast Atlantic Ocean. *Journal of Geophysical Research*, *117*(D6). <https://doi.org/10.1029/2011JD016773>
- Archer-Nicholls, S., Allen, R., Abraham, N. L., Griffiths, P. T., & Archibald, A. T. (2023). Large simulated future changes in the nitrate radical under the CMIP6 SSP scenarios: Implications for oxidation chemistry. *Atmospheric Chemistry and Physics*, *23*(10), 5801–5813. <https://doi.org/10.5194/acp-23-5801-2023>
- Archibald, A. T., O'Connor, F. M., Abraham, N. L., Archer-Nicholls, S., Chipperfield, M. P., Dalvi, M., et al. (2020). Description and evaluation of the UKCA stratosphere-troposphere chemistry scheme (StratTrop v1.0) implemented in UKESM1. *Geoscientific Model Development*, *13*(3), 1223–1266. <https://doi.org/10.5194/gmd-13-1223-2020>
- Bates, T. S., Cline, J. D., Gammon, R. H., & Kelly-Hansen, S. R. (1987). Regional and seasonal variations in the flux of oceanic dimethylsulfide to the atmosphere. *Journal of Geophysical Research*, *92*(C3), 2930–2938. <https://doi.org/10.1029/jc092i03p02930>
- Bauer, S. E., Tsigaridis, K., Faluvegi, G., Kelley, M., Lo, K. K., Miller, R. L., et al. (2020). Historical (1850–2014) aerosol evolution and role on climate forcing using the GISS ModelE2.1 contribution to CMIP6. *Journal of Advances in Modeling Earth Systems*, *12*(8), e2019MS001978. <https://doi.org/10.1029/2019MS001978>
- Belviso, S., Bopp, L., Moulin, C., Orr, J. C., Anderson, T., Aumont, O., et al. (2004). Comparison of global climatological maps of sea surface dimethyl sulfide. *Global Biogeochemical Cycles*, *18*(3). <https://doi.org/10.1029/2003GB002193>
- Bhatti, Y., Revell, L., & McDonald, A. (2022). Influences of Antarctic ozone depletion on Southern Ocean aerosols. *Journal of Geophysical Research: Atmospheres*, *127*(18), e2022JD037199. <https://doi.org/10.1029/2022JD037199>
- Bhatti, Y. A., Revell, L. E., Schuddeboom, A. J., McDonald, A. J., Archibald, A. T., Williams, J., et al. (2023). The sensitivity of Southern Ocean atmospheric dimethyl sulfide (DMS) to modeled oceanic DMS concentrations and emissions. *Atmospheric Chemistry and Physics*, *23*(24), 15181–15196. <https://doi.org/10.5194/acp-23-15181-2023>
- Blomquist, B. W., Brumer, S. E., Fairall, C. W., Huebert, B. J., Zappa, C. J., Brooks, I. M., et al. (2017). Wind speed and sea state dependencies of air-sea gas transfer: Results from the High Wind speed Gas exchange Study (HiWinGS). *Journal of Geophysical Research: Oceans*, *122*(10), 8034–8062. <https://doi.org/10.1002/2017jc013181>
- Bock, J., Michou, M., Nabat, P., Abe, M., Mulcahy, J. P., Olivie, D. J., et al. (2021). Evaluation of ocean dimethylsulfide concentration and emission in CMIP6 models. *Biogeosciences*, *18*(12), 3823–3860. <https://doi.org/10.5194/bg-18-3823-2021>
- Boucher, O., Moulin, C., Belviso, S., Aumont, O., Bopp, L., Cosme, E., et al. (2003). DMS atmospheric concentrations and sulphate aerosol indirect radiative forcing: A sensitivity study to the DMS source representation and oxidation. *Atmospheric Chemistry and Physics*, *3*(1), 49–65. <https://doi.org/10.5194/acp-3-49-2003>
- Breider, T. J., Chipperfield, M. P., Richards, N. A. D., Carslaw, K. S., Mann, G. W., & Spracklen, D. V. (2010). Impact of BrO on dimethylsulfide in the remote marine boundary layer. *Geophysical Research Letters*, *37*(2). <https://doi.org/10.1029/2009GL040868>
- Burkholder, J., Sander, S., Abbatt, J., Barker, J., Cappa, C., Crounse, J., et al. (2020). *Chemical kinetics and photochemical data for use in atmospheric studies; evaluation number 19* (Report). Jet Propulsion Laboratory, National Aeronautics and Space ...
- Cala, B. A., Archer-Nicholls, S., Weber, J., Abraham, N. L., Griffiths, P. T., Jacob, L., et al. (2023). Development, intercomparison and evaluation of an improved mechanism for the oxidation of dimethyl sulfide in the UKCA model. *Atmospheric Chemistry and Physics*, *23*(23), 1–51. <https://doi.org/10.5194/acp-23-14735-2023>
- Carslaw, K. S., Lee, L. A., Reddington, C. L., Pringle, K. J., Rap, A., Forster, P. M., et al. (2013). Large contribution of natural aerosols to uncertainty in indirect forcing. *Nature*, *503*(7474), 67–71. <https://doi.org/10.1038/nature12674>
- Charlson, R. J., Lovelock, J. E., Andreae, M. O., & Warren, S. G. (1987). Oceanic phytoplankton, atmospheric sulphur, cloud albedo and climate. *Nature*, *326*(6114), 655–661. <https://doi.org/10.1038/326655a0>
- Chen, Q., Geng, L., Schmidt, J. A., Xie, Z., Kang, H., Dachs, J., et al. (2016). Isotopic constraints on the role of hypohalous acids in sulfate aerosol formation in the remote marine boundary layer. *Atmospheric Chemistry and Physics*, *16*(17), 11433–11450. <https://doi.org/10.5194/acp-16-11433-2016>
- Chen, Q., Schmidt, J. A., Shah, V., Jaeglé, L., Sherwen, T., & Alexander, B. (2017). Sulfate production by reactive bromine: Implications for the global sulfur and reactive bromine budgets. *Geophysical Research Letters*, *44*(13), 7069–7078. <https://doi.org/10.1002/2017GL073812>
- Chen, Q., Sherwen, T., Evans, M., & Alexander, B. (2018). DMS oxidation and sulfur aerosol formation in the marine troposphere: A focus on reactive halogen and multiphase chemistry. *Atmospheric Chemistry and Physics*, *18*(18), 13617–13637. <https://doi.org/10.5194/acp-18-13617-2018>
- Chin, M., Jacob, D. J., Gardner, G. M., Foreman-Fowler, M. S., Spiro, P. A., & Savoie, D. L. (1996). A global three-dimensional model of tropospheric sulfate. *Journal of Geophysical Research*, *101*(D13), 18667–18690. <https://doi.org/10.1029/96JD01221>
- Curran, M. A., & Jones, G. B. (2000). Dimethyl sulfide in the Southern Ocean: Seasonality and flux. *Journal of Geophysical Research*, *105*(D16), 20451–20459. <https://doi.org/10.1029/2000jd900176>

- Dee, D. P., Uppala, S. M., Simmons, A. J., Berrisford, P., Poli, P., Kobayashi, S., et al. (2011). The ERA-interim reanalysis: Configuration and performance of the data assimilation system. *Quarterly Journal of the Royal Meteorological Society*, *137*(656), 553–597. <https://doi.org/10.1002/qj.828>
- Feinberg, A., Sukhodolov, T., Luo, B.-P., Rozanov, E., Winkel, L. H. E., Peter, T., & Stenke, A. (2019). Improved tropospheric and stratospheric sulfur cycle in the aerosol–chemistry–climate model SOCOL-AERv2. *Geoscientific Model Development*, *12*(9), 3863–3887. <https://doi.org/10.5194/gmd-12-3863-2019>
- Fiddes, S. L., Woodhouse, M. T., Nicholls, Z., Lane, T. P., & Schofield, R. (2018). Cloud, precipitation and radiation responses to large perturbations in global dimethyl sulfide. *Atmospheric Chemistry and Physics*, *18*(14), 10177–10198. <https://doi.org/10.5194/acp-18-10177-2018>
- Fung, K. M., Heald, C. L., Kroll, J. H., Wang, S., Jo, D. S., Gettelman, A., et al. (2022). Exploring dimethyl sulfide (DMS) oxidation and implications for global aerosol radiative forcing. *Atmospheric Chemistry and Physics*, *22*(2), 1549–1573. <https://doi.org/10.5194/acp-22-1549-2022>
- Gondwe, M., Krol, M., Gieskes, W., Klaassen, W., & de Baar, H. (2003). The contribution of ocean-leaving DMS to the global atmospheric burdens of DMS, MSA, SO₂, and NSS SO₄=. *Global Biogeochemical Cycles*, *17*(2). <https://doi.org/10.1029/2002gb001937>
- Grosvenor, D. P., Sourdeval, O., Zuidema, P., Ackerman, A., Alexandrov, M. D., Bennartz, R., et al. (2018). Remote sensing of droplet number concentration in warm clouds: A review of the current state of knowledge and perspectives [dataset]. *Reviews of Geophysics*, *56*(2), 409–453. <https://doi.org/10.1029/2017RG000593>
- Hamilton, D. S., Lee, L. A., Pringle, K. J., Reddington, C. L., Spracklen, D. V., & Carslaw, K. S. (2014). Occurrence of pristine aerosol environments on a polluted planet. *Proceedings of the National Academy of Sciences of the United States of America*, *111*(52), 18466–18471. <https://doi.org/10.1073/pnas.1415440111>
- Hardacre, C., Mulcahy, J. P., Pope, R. J., Jones, C. G., Rumbold, S. T., Li, C., et al. (2021). Evaluation of SO₂, SO₄²⁻ and an updated SO₂ dry deposition parameterization in the United Kingdom Earth System Model. *Atmospheric Chemistry and Physics*, *21*(24), 18465–18497. <https://doi.org/10.5194/acp-21-18465-2021>
- Hersbach, H., Bell, B., Berrisford, P., Hirahara, S., Horányi, A., Muñoz-Sabater, J., et al. (2020). The ERA5 global reanalysis. *Quarterly Journal of the Royal Meteorological Society*, *146*(730), 1999–2049. <https://doi.org/10.1002/qj.3803>
- Hoesly, R. M., Smith, S. J., Feng, L., Klimont, Z., Janssens-Maenhout, G., Pitkanen, T., et al. (2018). Historical (1750–2014) anthropogenic emissions of reactive gases and aerosols from the Community Emissions Data System (CEDS). *Geoscientific Model Development*, *11*(1), 369–408. <https://doi.org/10.5194/gmd-11-369-2018>
- Hoffmann, E. H., Heinold, B., Kubin, A., Tegen, I., & Herrmann, H. (2021). The importance of the representation of DMS oxidation in global chemistry–climate simulations. *Geophysical Research Letters*, *48*(13), e2021GL094068. <https://doi.org/10.1029/2021GL094068>
- Horowitz, L. W., Naik, V., Paulot, F., Ginoux, P. A., Dunne, J. P., Mao, J., et al. (2020). The GFDL global atmospheric chemistry–climate model AM4.1: Model description and simulation characteristics. *Journal of Advances in Modeling Earth Systems*, *12*(10), e2019MS002032. <https://doi.org/10.1029/2019MS002032>
- Hulswar, S., Simó, R., Gali Tapias, M., Bell, T. G., Lana, A., Inamdar, S., et al. (2022). Third revision of the global surface seawater dimethyl sulfide climatology (DMS-Rev3). *Earth System Science Data*, *14*(7), 2963–2987. <https://doi.org/10.5194/essd-14-2963-2022>
- Jarníková, T., & Tortell, P. D. (2016). Towards a revised climatology of summertime dimethylsulfide concentrations and sea–air fluxes in the Southern Ocean. *Environmental Chemistry*, *13*(2), 364. <https://doi.org/10.1071/EN14272>
- Keller, M. D., Bellows, W. K., & Guillard, R. R. (1989). Dimethyl sulfide production in marine phytoplankton. In *Biogenic sulfur in the environment* (Vol. 393, pp. 167–182). ACS Symposium Series. <https://doi.org/10.1021/bk-1989-0393.ch011>
- Kettle, A., & Andreae, M. (2000). Flux of dimethylsulfide from the oceans: A comparison of updated data sets and flux models. *Journal of Geophysical Research*, *105*(D22), 26793–26808. <https://doi.org/10.1029/2000jd900252>
- Kettle, A., Andreae, M. O., Amouroux, D., Andreae, T., Bates, T., Berresheim, H., et al. (1999). A global database of sea surface dimethylsulfide (DMS) measurements and a procedure to predict sea surface DMS as a function of latitude, longitude, and month. *Global Biogeochemical Cycles*, *13*(2), 399–444. <https://doi.org/10.1029/1999gb900004>
- Kirkevåg, A., Grini, A., Oliví, D., Seland, O., Alterskjær, K., Hummel, M., et al. (2018). A production-tagged aerosol module for Earth system models, OsloAero5.3 – Extensions and updates for CAM5.3-OSLO. *Geoscientific Model Development*, *11*(10), 3945–3982. <https://doi.org/10.5194/gmd-11-3945-2018>
- Kirkevåg, A., Iversen, T., Seland, O., Hoose, C., Kristjánsson, J. E., Struthers, H., et al. (2013). Aerosol–climate interactions in the Norwegian Earth System Model – NorESM1-M. *Geoscientific Model Development*, *6*(1), 207–244. <https://doi.org/10.5194/gmd-6-207-2013>
- Kloster, S., Feichter, J., Maier-Reimer, E., Six, K. D., Stier, P., & Wetzel, P. (2006). DMS cycle in the marine ocean–atmosphere system—a global model study. *Biogeosciences*, *3*(1), 29–51. <https://doi.org/10.5194/bg-3-29-2006>
- Korhonen, H., Carslaw, K. S., Spracklen, D. V., Mann, G. W., & Woodhouse, M. T. (2008). Influence of oceanic dimethyl sulfide emissions on cloud condensation nuclei concentrations and seasonality over the remote Southern Hemisphere oceans: A global model study. *Journal of Geophysical Research*, *113*(D15). <https://doi.org/10.1029/2007jd009718>
- Krasting, J. P., John, J. G., Blanton, C., McHugh, C., Nikonov, S., Radhakrishnan, A., et al. (2018). NOAA-GFDL GFDL-ESM4 model output prepared for CMIP6 CMIP historical [dataset]. Earth System Grid Federation. <https://doi.org/10.22033/ESGF/CMIP6.8597>
- Lana, A., Bell, T., Simó, R., Vallina, S., Ballabrera-Poy, J., Kettle, A., et al. (2011). An updated climatology of surface dimethylsulfide concentrations and emission fluxes in the global ocean. *Global Biogeochemical Cycles*, *25*(1). <https://doi.org/10.1029/2010gb003850>
- Loeb, N. G., Doelling, D. R., Wang, H., Su, W., Nguyen, C., Corbett, J. G., et al. (2018). Clouds and the Earth’s Radiant Energy System (CERES) Energy Balanced and Filled (EBAF) Top-of-Atmosphere (TOA) Edition-4.0 data product [dataset]. *Journal of Climate*, *31*(2), 895–918. <https://doi.org/10.1175/JCLI-D-17-0208.1>
- Lovelock, J. E., Maggs, R. J., & Rasmussen, R. A. (1972). Atmospheric dimethyl sulphide and the natural sulphur cycle. *Nature*, *237*(5356), 452–453. <https://doi.org/10.1038/237452a0>
- McCoy, I. L., McCoy, D. T., Wood, R., Regayre, L., Watson-Parris, D., Grosvenor, D. P., et al. (2020). The hemispheric contrast in cloud microphysical properties constrains aerosol forcing. *Proceedings of the National Academy of Sciences of the United States of America*, *117*(32), 18998–19006. <https://doi.org/10.1073/pnas.1922502117>
- Minikin, A., Petzold, A., Ström, J., Krejci, R., Seifert, M., van Velthoven, P., et al. (2003). Aircraft observations of the upper tropospheric fine particle aerosol in the Northern and Southern Hemispheres at midlatitudes. *Geophysical Research Letters*, *30*(10). <https://doi.org/10.1029/2002GL016458>
- Mulcahy, J. P., Johnson, C., Jones, C. G., Povey, A. C., Scott, C. E., Sellar, A., et al. (2020). Description and evaluation of aerosol in UKESM1 and HadGEM3-GC3.1 CMIP6 historical simulations. *Geoscientific Model Development*, *13*(12), 6383–6423. <https://doi.org/10.5194/gmd-13-6383-2020>

- Neely, R. R. III, & Schmidt, A. (2016). VolcanEESM: Global volcanic sulphur dioxide (SO₂) emissions database from 1850 to present - Version 1.0 [object Object]. <https://doi.org/10.5285/76EBDC0B-0EED-4F70-B89E-55E606BCD568>
- Platnick, S., Meyer, K. G., King, M. D., Wind, G., Amarasinghe, N., Marchant, B., et al. (2017). The MODIS cloud optical and microphysical products: Collection 6 updates and examples from Terra and Aqua. *IEEE Transactions on Geoscience and Remote Sensing: A Publication of the IEEE Geoscience and Remote Sensing Society*, 55(1), 502–525. <https://doi.org/10.1109/TGRS.2016.2610522>
- Revell, L. E., Kremser, S., Hartery, S., Harvey, M., Mulcahy, J. P., Williams, J., et al. (2019). The sensitivity of Southern Ocean aerosols and cloud microphysics to sea spray and sulfate aerosol production in the HadGEM3-GA7. 1 chemistry–climate model. *Atmospheric Chemistry and Physics*, 19(24), 15447–15466. <https://doi.org/10.5194/acp-19-15447-2019>
- Sellar, A. A., Jones, C. G., Mulcahy, J. P., Tang, Y., Yool, A., Wiltshire, A., et al. (2019). UKESM1: Description and evaluation of the UK Earth System Model. *Journal of Advances in Modeling Earth Systems*, 11(12), 4513–4558. <https://doi.org/10.1029/2019ms001739>
- Seo, J., Shim, S., Kwon, S.-H., Boo, K.-O., Kim, Y.-H., O'Connor, F., et al. (2020). The impacts of aerosol emissions on historical climate in UKESM1. *Atmosphere*, 11(10), 1095. <https://doi.org/10.3390/atmos11101095>
- Shah, V., Jacob, D. J., Moch, J. M., Wang, X., & Zhai, S. (2020). Global modeling of cloud water acidity, precipitation acidity, and acid inputs to ecosystems. *Atmospheric Chemistry and Physics*, 20(20), 12223–12245. <https://doi.org/10.5194/acp-20-12223-2020>
- Sheng, J.-X., Weisenstein, D. K., Luo, B.-P., Rozanov, E., Stenke, A., Anet, J., et al. (2015). Global atmospheric sulfur budget under volcanically quiescent conditions: Aerosol-chemistry-climate model predictions and validation. *Journal of Geophysical Research: Atmospheres*, 120(1), 256–276. <https://doi.org/10.1002/2014JD021985>
- Smith, S. J., van Aardenne, J., Klimont, Z., Andres, R. J., Volke, A., & Delgado Arias, S. (2011). Anthropogenic sulfur dioxide emissions: 1850–2005. *Atmospheric Chemistry and Physics*, 11(3), 1101–1116. <https://doi.org/10.5194/acp-11-1101-2011>
- Szopa, S., Naik, V., Adhikary, B., Artaxo, P., Bernsten, T., Collins, W. D., et al. (2021). Short-lived climate forcers. In *Climate change 2021: The physical science basis. Contribution of working group I to the sixth assessment report of the intergovernmental panel on climate change* (pp. 817–922). Cambridge University Press. <https://doi.org/10.1017/9781009157896.008>
- Tashmim, L., Porter, W. C., Chen, Q., Alexander, B., Fite, C. H., Holmes, C. D., et al. (2024). Contribution of expanded marine sulfur chemistry to the seasonal variability of dimethyl sulfide oxidation products and size-resolved sulfate aerosol. *Atmospheric Chemistry and Physics*, 24(6), 3379–3403. <https://doi.org/10.5194/acp-24-3379-2024>
- Tsigaridis, K., Krol, M., Dentener, F. J., Balkanski, Y., Lathière, J., Metzger, S., et al. (2006). Change in global aerosol composition since preindustrial times. *Atmospheric Chemistry and Physics*, 6(12), 5143–5162. <https://doi.org/10.5194/acp-6-5143-2006>
- Turnock, S. T., Allen, R. J., Andrews, M., Bauer, S. E., Deushi, M., Emmons, L., et al. (2020). Historical and future changes in air pollutants from CMIP6 models. *Atmospheric Chemistry and Physics*, 20(23), 14547–14579. <https://doi.org/10.5194/acp-20-14547-2020>
- Turnock, S. T., Butt, E. W., Richardson, T. B., Mann, G. W., Reddington, C. L., Forster, P. M., et al. (2016). The impact of European legislative and technology measures to reduce air pollutants on air quality, human health and climate. *Environmental Research Letters*, 11(2), 024010. <https://doi.org/10.1088/1748-9326/11/2/024010>
- Turnock, S. T., Mann, G. W., Woodhouse, M. T., Dalvi, M., O'Connor, F. M., Carslaw, K. S., & Spracklen, D. V. (2019). The impact of changes in cloud water pH on aerosol radiative forcing. *Geophysical Research Letters*, 46(7), 4039–4048. <https://doi.org/10.1029/2019GL082067>
- van Marle, M. J., Kloster, S., Magi, B. I., Marlon, J. R., Daniau, A.-L., Field, R. D., et al. (2016). Biomass Burning emissions for CMIP6 (v1.2). *Earth System Grid Federation*. <https://doi.org/10.22033/ESGF/input4MIPs.1117>
- Veres, P. R., Neuman, J. A., Bertram, T. H., Assaf, E., Wolfe, G. M., Williamson, C. J., et al. (2020). Global airborne sampling reveals a previously unobserved dimethyl sulfide oxidation mechanism in the marine atmosphere. *Proceedings of the National Academy of Sciences of the United States of America*, 117(9), 4505–4510. <https://doi.org/10.1073/pnas.1919344117>
- Vogel, A., Alessa, G., Scheele, R., Weber, L., Dubovik, O., North, P., & Fiedler, S. (2022). Uncertainty in aerosol optical depth from modern aerosol-climate models, reanalyses, and satellite products. *Journal of Geophysical Research: Atmospheres*, 127(2), e2021JD035483. <https://doi.org/10.1029/2021JD035483>
- Walters, D., Baran, A. J., Boutle, I., Brooks, M., Earnshaw, P., Edwards, J., et al. (2019). The Met Office unified model global atmosphere 7.0/7.1 and JULES global land 7.0 configurations. *Geoscientific Model Development*, 12(5), 1909–1963. <https://doi.org/10.5194/gmd-12-1909-2019>